Biophysical Journal, volume 99

Supporting Material for:

Bidirectional power stroke by ncd kinesin

Anthony E. Butterfield[1], Russell J. Stewart[2], Christoph F. Schmidt[3], and Mikhail Skliar[1]

[1] Department of Chemical Engineering, University of Utah, Salt Lake City, UT 84112, USA

[2] Department of Bioengineering, University of Utah, Salt Lake City, UT 84112, USA

[3] Fakultät für Physik, Drittes Physikalisches Institut, Georg-August-Universität Göttingen, 37077 Göttingen, Germany

Correspondence to:

A. E. Butterfield (tony3.1416@gmail.com) and M. Skliar (mikhail.skliar@utah.edu), 50 S. Central Campus Drive, Room MEB 3290, Salt Lake City, UT 84112.

Table S1 – Nomenclature

A	System matrix of the state space model
B	Input matrix of the state space model
C	Output matrix of the state space model
$d_{i,j}$	j^{th} motor head displacement within i^{th} attachment event
F_{AT}	Interaction force between ncd and the MT
G	Noise weighting matrix in Equation (6)
k	Boltzmann's constant
K_{TL} (K_{TR})	Optical trap spring constant for the left (right) bead
K_{LL} (K_{LR})	Spring constant of left (right) bead-MT attachment
K_L	Value of K_{LL} when $K_{LL} = K_{LR}$
K_{AT}	Spring constant of the ncd-MT attachment
K_{total}	Spring constant used in the single bead model
m_R (m_L)	Mass of the right (left) bead
m_R^{SB}	Mass of the bead in the single bead model
T	Temperature
u	Input vector of the state space model
v	Vector of measurement noises in the state space model
w	Vector of stochastic disturbances in the state space model
w_{AT}	Stochastic disturbance in the estimation of the motor head displacement
w_{FR} (w_{FL})	Stochastic disturbance used to model Brownian forces on the right (left) bead
w_{VR} (w_{VL})	Stochastic disturbance affecting the velocity of the right (left) bead
w_{FM}	Stochastic disturbance used to model Brownian forces on the MT
w_{total}	Stochastic disturbance used to parameterize the K_{total} model
x	State vector of the state space model
x_R (x_L)	Right (left) bead displacement
x_M	MT's mean equilibrium displacement
x_{AT}	Motor head displacement
x_{TR} (x_{TL})	Right (left) optical trap displacement
x_{tm}	Terminal motor head displacement
x_{eq}	Equilibrium motor head displacement
y	Measurement vector of the state space model
$\beta_R(\beta_L)$	Drag coefficient on the right (left) bead

TABLE S2

SUMMARY OF POWER STROKE CHARACTERIZATION

Method	Kalman-filtered data, syntactic classification	Ensemble-averaged (syntactic classification) then Kalman-filtered data,	Ensemble-averaged (NN classification) then Kalman-filtered data
Events with minus-end directed strokes	418 (62%)	418 (62%)	414 (61%)
Events with plus-end directed strokes	216 (32%)	216 (32%)	205 (30%)
Average amplitude of minus-end directed strokes (nm)	8.1	11.5	11.7
Average amplitude of plus-end directed strokes (nm)	6.4	7.4	7.3

Confirmation by Neural Network Classification

Specifically, radial-basis neural networks were designed and trained with synthetic data to classify motor events into different event types. These neural networks have two layers. A hidden layer contains radial basis neurons, represented by the transfer function $F=e^{-n^2}$. The output layer consists of linear neurons. The weights and biases of each neuron in the hidden layer determine the output of the network. The linear output neurons give the weighted sum of the radial basis functions. When applied to the training data (e.g., the synthetic right bead position measurements, example of which is given in Fig. 2), this method adds neurons to the hidden layer until the mean squared error satisfies the selected tolerance. The raw (unfiltered) optical trap measurements of x_R during all detected ncd-MT attachments were then fed to NN classifiers and the classification results were compared with those obtained using the model-based methods. When used with synthetic measurements, syntactic and neural network (NN) classifications have shown better than 95% accuracy in classifying motor events into the appropriate category. When applied to the experimental data, the neural networks classified 80% of all events into the same equilibrium displacement category, positive or negative, as the syntactic classification method (Fig. S1) used to produce the results of Table I. The vast majority of discrepancies occurred with equilibrium displacements of less than 10 nm. Overall, 47% of events were determined to have positive equilibrium displacements by the NN classification.

A slightly higher disagreement was observed in classifying terminal displacements, with 78% of events classified into the same categories. A lower agreement is expected since terminal displacements are classified based on only short segments of measurement data (~200 ms long) at the end of the attachment events, compared to the up to 2 s segments used to classify equilibrium displacements. Furthermore, unlike the more quantitative syntactic method of Fig. S1, which allows for a category of events with no terminal motor action, the NN classification assigned all events into either a positive or negative terminal displacement category, contributing to higher overall disagreement.

The neural networks classified optical trap data into 66% of motor events terminating with the minus-directed stroke and the remaining 34% of events as ending with the stroke towards the

plus end of the MT, in good agreement with the results of Table I. When the sign of the experimental data was reversed before applying NN classification, 30% of events were found to have minus-directed strokes. Although ideally we would expect to see 34% as the outcome, the test confirms that the designed neural networks discriminate reasonably well between positive and negative terminal motor actions.

Overall, both classification methods produced consistent results that indicate the presence of unexpected ncd power strokes towards the plus end of the MT. We deem the syntactic results to be more accurate compared to the NN classification, which utilizes unfiltered measurements of low signal-to-noise ratio to segregate events into different types.

Sources of uncertainty and sensitivity to model parameters

Since the results reported here are based on several MT-ncd constructs, it is interesting to ask what effect the different values of the model parameters (e.g. the spring stiffnesses) have on the results of the model-based filtering. We observed that the value of K_{total}, which depends on all spring constants, did not change significantly from experiment to experiment during attached and unattached time intervals. It remained practically constant throughout a single experiment. A sensitivity analysis using computer simulations indicated that changes in the spring constants, which correspond to the observed small changes in the estimated K_{total}, could result in no more than a nanometer difference in the estimated motor head displacement for different experiments. Overall, we conclude that parameter variability between the experiments did not significantly affect our results.

In addition to parameter variability, another source of model uncertainty is the unknown relationship between the compliance of the ncd-MT attachment and the relative motor-microtubule displacements. The compliance of bead-MT links is known to be nonlinear (van Mameren, J., Vermeulen, K. C., Gittes, F. & Schmidt, C. F. Leveraging Single Protein Polymers To Measure Flexural Rigidity. Journal of Physical Chemistry B 113, 3837-3844 (2009)). For simplicity we assume linearity, which is a good approximation given the small power strokes. The similarity between acquired and synthetic data produced using our models supports this assumption.

The Kalman filter is fairly robust to modeling uncertainties. Such robustness is due to the use of two kinds of information: the actual measurements and prior knowledge of the process expressed in the model. As a result, the Kalman filter typically produces better results than could be obtained using traditional (not model based) filtering methods or using the model predictions alone. As an illustration of this feature, we applied Kalman filtering and the method of equipartition (a method previously used to analyze the results of three-bead optical trap experiments) to estimate K_{total} from the synthetic data. We found that the Kalman filter more accurately estimated K_{total}, even though the single-bead model used in this filter is only an approximation of the two-bead model used to generate the data.

Summary of the Data Analysis

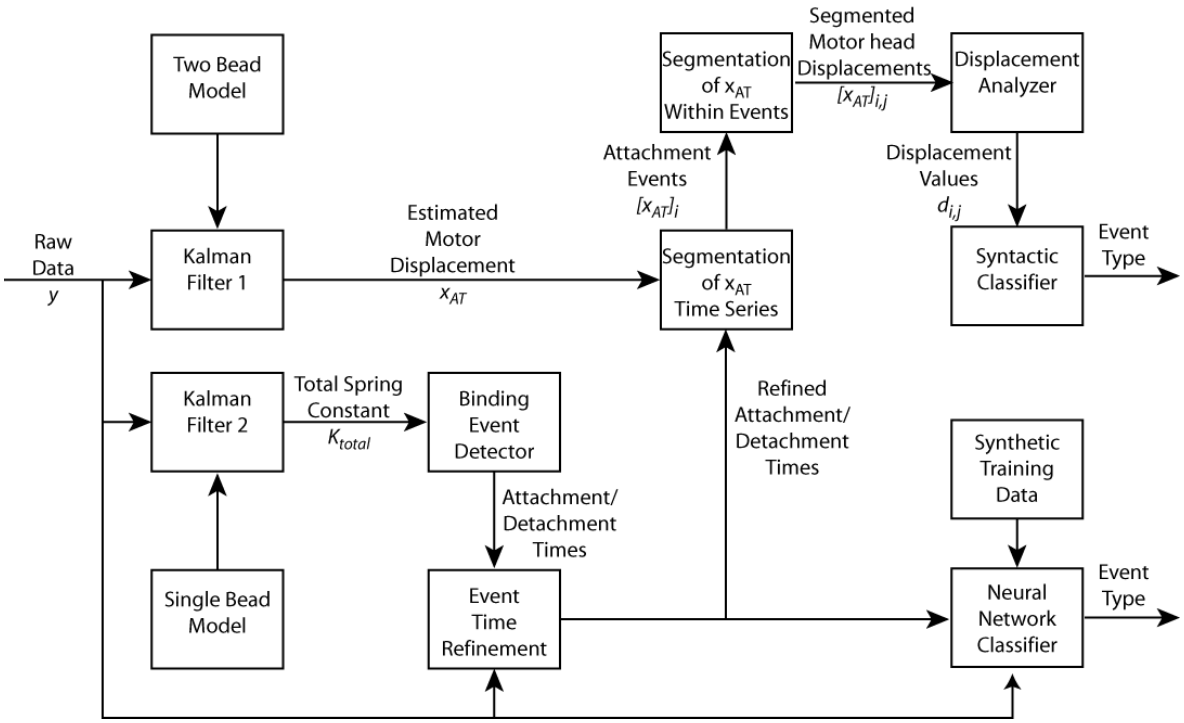

Figure S1: Summary of the filtering, identification, and syntactic event characterization process.

The following steps, indicated by their functionality, give additional details on the data analysis method summarized in Figure S1.

Pseudo-code 1. <u>De-trend data.</u>

De-trend measurements of the handle bead position, x_R, to remove measurement drift. De-trended measurements are used as the input **y** of single- and two-bead Kalman filters (Filters 1 and 2 in Fig. S1).

Pseudo-code 2. <u>Filter **y** and estimate motor head displacement, x_{AT}.</u>

Use Filter 1 to estimate the state vector **x** *(*of which x_{AT} is a component) and filter **y**. Our filter implementation is equivalent to the Kalman filter in Matlab's Control Systems Toolbox with: (a) the state space model defined by matrices *A* (Equation 8), *B* equal to 5x2 zero matrix, *G* given by Equation (9), and *C*=[1 0 0 0 0]; and (b) the covariances of the process and measurement noises, the selection of which is described in the Filter Validation section. Figure 4 shows several segments of **y** (shown in grey), the filtered measurements of the right bead position (filtered *y*; shown in green), and the estimated x_{AT} (blue line).

Pseudo-code 3. <u>Segment x_{AT} into ncd-MT attachment events.</u>

The total spring constant, K_{total}, is estimated next. Since the system matrix given by Equation (11) depends on K_{total}, the single-bead model is nonlinear. Therefore, the total spring constant is estimated using an extended Kalman filter (Filter 2),

which is a Kalman filter for a linearized model, where the linearization is continuously updated for the latest estimate of K_{total}. Figure 4 shows several segments of the estimated values of K_{total} (red line).

The Shewhart Control Chart method is then used to segment the identified K_{total} time series into the segments where K_{total} is elevated, which correspond to ncd-MT attachment events. The obtained ncd attachment and detachment times ($[t_a]_i$ and $[t_d]_i$ for the i^{th} attachment event) are then refined using a computationally more expensive variance windowing. The refined $[t_a]_i$ and $[t_d]_i$ segment the identified motor-head displacements, x_{AT}, into attachment events.

Pseudo-code 4. Determine x_{eq} and x_{tm} and event types.

For the i^{th} attachment event, framed by $[t_a]_i$ and $[t_d]_i$, the corresponding segment of the identified motor-head displacements is broken down into equilibrium and terminal displacements, x_{eq} and x_{tm}, by the instants of the rapid change in x_{AT}. Events are then classified (Syntactic Classifier in Fig. S1) as a positive or negative terminal displacement depending upon the difference in x_{tm} and x_{eq}. After averaging over all events and events of different types, the values are reported in Table 1.

Pseudo-code 5. Ensemble averaged measurements.

De-trended right bead position measurements, y, segmented and lined up by attachment and detachment times $[t_a]_i$ and $[t_d]$ are ensemble averaged for all events and different event types. The results are shown in Figure 5 as grey lines.

Pseudo-code 6. Estimate x_{AT} based on ensemble averaged measurements.

The motor head displacement is estimated using the two-bead Kalman filter with the ensemble averaged right bead measurements (Pseudo-code 5) as the input. Compared to the filter of Pseudo-code 2, a smaller covariance value of the measurement noise is used to reflect the reduction in thermal fluctuations achieved with averaging. A smaller covariance of the measurement noise results in a more aggressive filter with the higher Kalman gain. The result (estimated x_{AT}) is shown in Figure 5 as a black line.

Pseudo-code 7. Neural Network Confirmation.

A radial basis neural network was trained using simulated motor events. The trained network is then applied to the raw experimental data. Each event is given a positive or negative score by the network in order to classify events as having a positive or negative equilibrium and terminal displacements. The classification results are then used to average the measurements, providing an alternative to the result obtained with syntactic classification (Pseudo-code 4). These averaged measurements, when used as the input in Pseudo-code 6, lead to the motor-head displacement estimation shown in Figure 5 in light grey.